Graefes Arch Clin Exp Ophthalmol (2013) 251:1587–1592
DOI 10.1007/s00417-013-2285-8

GLAUCOMA

Assessment of trabecular meshwork width using swept source optical coherence tomography

Tin A. Tun · Mani Baskaran · Ce Zheng · Lisandro M. Sakata · Shamira A. Perera · Anita S. Chan · David S. Friedman · Carol Y. Cheung · Tin Aung

Received: 5 November 2012 / Revised: 3 January 2013 / Accepted: 7 February 2013 / Published online: 23 February 2013

Abstract
Purpose Measurements of the angle width by ultrasound biomicroscopy or anterior segment optical coherence tomography are usually performed 500 μm from the scleral spur, as the anterior part of trabecular meshwork (TM) is assumed to lie within this distance. The aim of this study was to measure TM width using swept source optical coherence tomography (SS-OCT, CASIA SS-1000, Tomey Corporation, Nagoya, Japan), and to investigate factors influencing this measurement.
Methods Participants underwent gonioscopy and SS-OCT imaging in the dark. High-definition SS-OCT images were corrected for refractive distortion; and customized software (ImageJ; National Institutes of Health, Bethesda, MD, USA) was utilized to measure TM width (distance between the scleral spur and Schwalbe's line). Linear regression analysis was performed to assess the relationship between TM width with demographic and angle parameters.
Results One hundred and forty eight Chinese subjects were analyzed. The majority was female (62.4 %); the mean age was 59.2±8.68 years. Identification of the scleral spur and Schwalbe's line with SS-OCT was possible in 590 (99.7 %) and 585 angle quadrants (98.8 %) respectively. TM width was wider in the inferior and superior quadrants (mean 889 [SD 138] and 793 [136] μm), compared to the nasal and temporal quadrants (712 [137] and 724 [115] μm, $P<0.001$). There was a difference in average TM width between open (789 [100]) and closed angle eyes (753 [86]) ($P=0.048$). There was no significant association between TM width and angle parameters, laterality, or demographic factors.
Conclusions In SS-OCT HD images, the mean TM width varied from 710 to 890 μm in the different quadrants of the eye, and the inferior quadrant TM was the widest compared to other quadrants.

Keywords Trabecular meshwork · Swept source optical coherence tomography · Quantitative angle measurements · Angle closure

T. A. Tun · M. Baskaran · C. Zheng · S. A. Perera · A. S. Chan · C. Y. Cheung · T. Aung (✉)
Singapore Eye Research Institute and Singapore National Eye Centre, 11 Third Hospital Avenue,
Singapore 168751, Singapore
e-mail: aung.tin@snec.com.sg

M. Baskaran · C. Zheng · C. Y. Cheung · T. Aung
Yong Loo Lin School of Medicine, National University of Singapore, Singapore, Singapore

M. Baskaran · C. Y. Cheung · T. Aung
Duke-NUS Graduate Medical School, National University of Singapore, Singapore, Singapore

C. Zheng
Joint Shantou International Eye Center of Shantou University and the Chinese University of Hong Kong, MA Liu Shui, Hong Kong

L. M. Sakata
Federal University of Parana, Curitiba, Brazil

A. S. Chan
Department of Pathology, Singapore General Hospital, Outram Park, Singapore

D. S. Friedman
Wilmer Eye Institute, Dana Center for Preventive Ophthalmology, Johns Hopkins University, Baltimore, MD, USA

Introduction

Anterior segment imaging techniques [1] such as ultrasound biomicroscopy, Scheimpflug photography, and anterior segment optical coherence tomography provide objective documentation of the angle [2, 3], as opposed to the subjective evaluation using gonioscopy. A major limitation of the imaging devices, however, is the inability to correctly

identify the location and extent of the trabecular meshwork which is the major site of aqueous outflow.

Optical coherence tomography (OCT) technology has evolved from time-domain to Fourier-domain or spectral-domain systems, with enhanced signal-to-noise ratio, image acquisition speed, and resolution [4]. Fourier-domain systems yield A-scan rates from 20 kHz (spectral-domain) [5] to 400 kHz (swept-source) [6], and are capable of 3-dimensional imaging of biological structures. There are at least eight commercially available spectral-domain OCT (SD-OCT) devices for optic disc and macular imaging, but only a few are able to image the anterior segment. Swept-source OCT (SS-OCT, CASIA SS-1000, Tomey Corporation, Nagoya, Japan) is a variation of Fourier-domain OCT that employs a monochromatic tunable fast scanning laser source, and a photodetector to receive wavelength resolved interference signal [7, 8]. The device is specifically designed for anterior segment imaging using 1,310 nm wavelength with a scan speed of 30,000 A-scans per second, with an axial resolution of less than 10 μm. There are two types of 3-dimensional (3D) scan protocols, a low-density scan (3D angle analysis scan, dimension, 16 mm × 6 mm) reconstructed from 128 radial scans, and a high-definition scan (3D angle HD scan, dimension, 8 mm × 4 mm) from 64 radial scans.

In the high-definition scan mode, both the scleral spur (SS) and the Schwalbe's line (SL) can be identified [9]. These structures represent anatomical landmarks that determine the boundaries of the TM. Previously published ultrasound biomicroscopy or anterior segment OCT measures of angle width have relied on measures taken at a fixed distance from the scleral spur [10, 11]. The distances selected were based on published data indicating that a point located 250 μm from the scleral spur along the angle wall would fall on the posterior trabecular meshwork, and a point located 500 μm would fall on the anterior part of the trabecular meshwork [11]. These assumptions have not been confirmed. The purpose of this study was to evaluate the TM width in different quadrants of the eye with SS-OCT, and to investigate factors influencing this measurement.

Methods

One hundred and sixty study participants were recruited from glaucoma clinics at Singapore National Eye Centre, Singapore. Written informed consent was obtained from all subjects. The study had the approval of the institutional review board of the Singapore Eye Research Institute, and adhered to the tenets of the Declaration of Helsinki. Of 160 participants, six (3.75 %) subjects were excluded for incomplete imaging data, and another six were excluded as they were non-Chinese.

All subjects underwent a standardized examination that included measurement of visual acuity, anterior segment imaging by SS-OCT, slit-lamp biomicroscopy, Goldmann applanation tonometry, and dark-room gonioscopy on the same day. Subjects with a history of intraocular surgery or penetrating trauma, or those with any corneal abnormalities that would preclude gonioscopy or imaging, were excluded from the study, but patients with previous laser iridotomy were included. Those with peripheral anterior synechiae were excluded.

Gonioscopy

A single masked examiner with glaucoma fellowship training (MB) performed gonioscopy in the dark for all subjects using a Sussman four-mirror lens (Ocular instruments Inc., Bellevue, WA, USA). The angle in each quadrant was graded using the modified Shaffer grading system, based on the anatomical structures observed during gonioscopy (grade 0=no angle structures, grade 1=Schwalbe's line, grade 2=anterior trabecular meshwork, grade 3=posterior trabecular meshwork or scleral spur, grade 4=visible ciliary body band). A quadrant was considered "closed" if the posterior trabecular meshwork could not be seen in the primary position without indentation (modified Shaffer grade 0, 1 or 2). Angle closure in an eye was defined as having two or more closed quadrants.

Angle imaging

One randomly selected eye was imaged using the 3D-angle high definition (HD) scan protocol of the SS-OCT under dark room conditions before any procedures involving contact with the eye. The 3D-angle HD protocol is a volumetric scan (dimension, 8 mm × 4 mm and 64 B scans), and takes 1.2 s. A subset of 29 patients (20 % of sample size) was imaged bilaterally to assess for differences between eyes. Seated subjects were directed to look at one of four peripheral fixation targets (up, down, right, and left) so that the iridocorneal angle was centered in the instrument's field of view. The operator had to open the eyelid when examining the superior and inferior quadrants, taking care to avoid pressing on the globe. Each image was averaged automatically from three consecutive scans by the manufacturer's software. Subsequently, we manually chose only the images centered at 3, 6, 9, and 12 o'clock positions from the 64 scans for image analysis.

Image analysis

A single masked examiner (TAT) graded the SS-OCT images. The scans were adjusted for refraction distortion at the air–corneal interface using the CASIA built-in program. We used our own customized software [the Anterior Segment Analysis

Table 1 Quadrant-wise visibility of anterior chamber angle structures (n=592 quadrants)

Quadrant	Schwalbe's line Visible n (%)	Scleral Spur Visible n (%)
Inferior	145 (98)	147 (99.3)
Superior	144 (97.3)	147 (99.3)
Nasal	148 (100)	148 (100)
Temporal	148 (100)	148 (100)
Total	585 (98.8)	590 (99.7)

Program (ASAP)] to measure angle structures. ASAP uses Image J (version 1.410), a public-domain Java program (available at http://rsb.info.nih.gov/ij; National Institutes of Health, Bethesda, MD, USA). ASAP was utilized to measure the TM width and conventional angle parameters (AOD500, AOD750, TISA500, and TISA750 from scleral spur). The ASAP algorithm calculated all parameters automatically after the observer marked the location of the scleral spur and Schwalbe's line. The scleral spur was defined as an inward projection of sclera, where the internal surface of cornea and sclera meet. Schwalbe's line was defined as the termination of endothelium or Descemet's membrane.

A subset of 20 images (ten with open-angle and ten with closed-angle) were randomly selected for reproducibility studies. Two observers (TAT and CZ) independently measured the 20 images to determine the inter-observer reproducibility of TM width. One observer (TAT) repeated the TM measurements after 2 weeks to determine the intra-observer reproducibility of TM width. Both observers were masked to gonioscopy and clinical findings.

Statistical analysis

Statistical analyses were performed using MedCalc, Windows v12.0, Mariakerke, Belgium. Continuous variables were described as the mean, standard deviation, and range. We used stepwise multiple linear regression analysis to assess the relationship of TM width with age, gender, angle status, and conventional angle parameters. We used one way analysis of variance (ANOVA) with the Student–Newman–Keuls method [12] for quadrant-wise TM width comparisons. We used independent sample t-test to compare TM widths between quadrants. We used paired sample t-test to compare findings between eyes of the same individual. Inter- and intra-observer reproducibility was assessed for TM width by using Bland–Altman analysis. Statistical significance was set at $P<0.05$.

Results

Of 160 participants, 12 subjects were excluded, leaving 148 subjects of Chinese ethnicity in the final analysis. The visibility of angle structures on SS-OCT images was as follows: scleral spur (590/592 quadrants, 99.7 %) and Schwalbe's line (585/592, 98.8 %, Table 1). Both structures were visible in all nasal and temporal quadrants. Further analysis was performed in 141 subjects [after excluding an additional seven subjects (4.38 %) due to poor image quality] in whom angle structures were visible in all four quadrants. There were more females (88/141, 62.4 %) than males, and more subjects with open angles (447/592, 75.5 %). There were 107 normal eyes (75.9 %), 31 (22 %) with primary angle closure suspects, one (0.7 %) with primary angle closure, one with primary angle closure glaucoma, and one with primary open-angle glaucoma.

The mean (SD) TM width was 779 (98) μm (range 554 to 1,054 μm). TM width was wider in the inferior and superior quadrants (mean 889 [SD 138] and 793 [136] μm), compared to the nasal and temporal quadrants (712 [137] and 724 [115] μm, $P<0.001$). All the TM width differences were statistically significant, with the exception of the comparison between nasal and temporal quadrants ($P=0.99$). Table 2 shows the difference in TM width among the four quadrants of the eye in the whole study sample, and also separately in eyes with open and closed angles. Average TM width was wider in open-angle eyes compared to closed

Table 2 Comparison of trabecular meshwork width in different quadrants and between eyes with open and closed angles

Quadrant	Overall (n=141)* Mean TM width in μm (SD)	Open angles (n=102) Mean TM width in μm (SD)	Closed angles (n=39) Mean TM width in μm (SD)	P-value(t-test)
Superior	793 (136)	793 (140)	792 (129)	0.98
Nasal	712 (137)	717 (142)	698 (122)	0.462
Temporal	724 (115)	734 (116)	696 (108)	0.089
Inferior	889 (138)	899 (137)	844 (134)	0.065
Mean	779 (98)	789 (100)**	753 (86)**	0.048

*Student–Newman–Keuls multiple comparisons between quadrants of the whole study sample showed significance $P<0.001$, except between nasal and temporal quadrants

**Stepwise multiple regression analysis of average TM width between open and closed angles, $P<0.05$

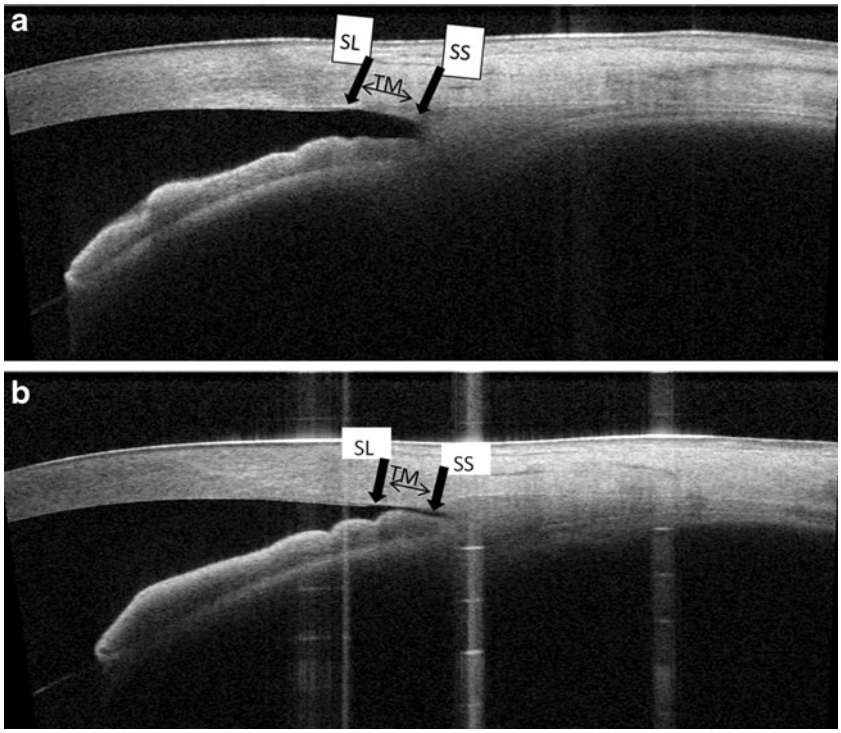

Fig. 1 Swept–source optical coherence tomography high definition images showing angle structures. **a** An open angle **b** A closed angle

angles (P=0.048). Figure 1a and b illustrates open- and closed–angle SS-OCT images. Figure 2a and b demonstrates angle measurements using ASAP software.

TM width was not associated with sex (beta=−0.019, P=0.28), age (beta=−0.001, P=0.33) or conventional angle parameters (beta=0.35, P=0.68). In the subset of 29 eyes imaged bilaterally, there was no difference in the TM width of right eyes [751 (80) μm] and left eyes [729 (89) μm, P= 0.35]. The mean difference for intra-observer reproducibility for TM width measurement was 0.029 μm [−0.132, 0.19 (95 % limits of agreement)] and for inter-observer reproducibility was 0.035 μm [−0.164, 0.234 (95 % limits of agreement)].

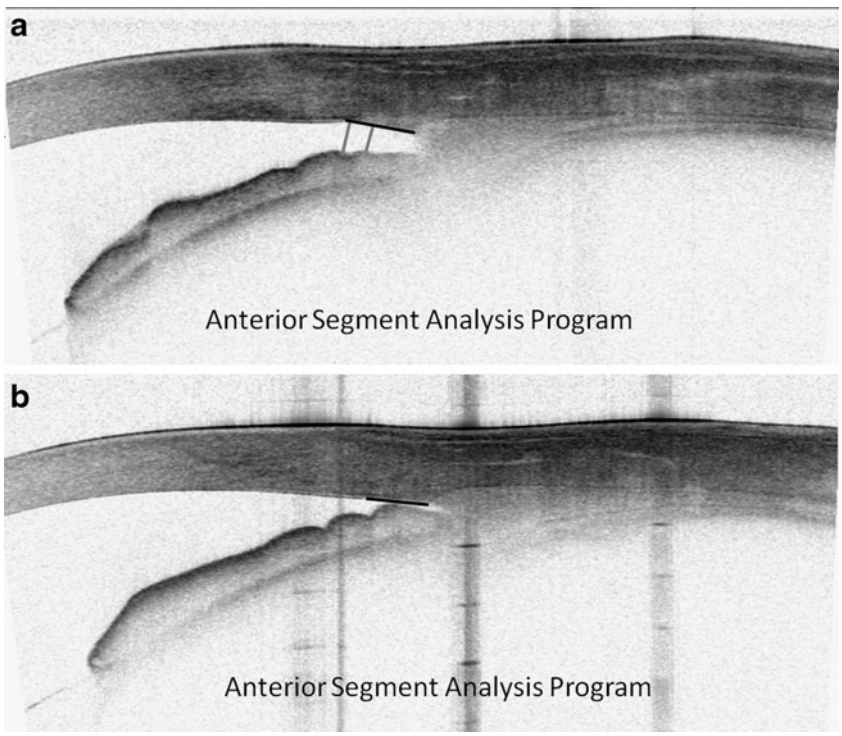

Fig. 2 Measurement of TM width and conventional angle parameters using ASAP. **a** An open angle. *Black line* indicates TM, *gray lines* — AOD 500 and AOD 750, **b** A closed angle. *Black line* indicates TM

Discussion

We found that the mean TM width was 779 (SD 98) μm (range 554 to 1,054 μm), with longer TM in the superior and inferior angles than in the nasal and temporal ones. Our results suggest that the previously used cutoff point of 500 μm from the scleral spur may need to be reconsidered, since TM is still present more anteriorly. Others have also reported that the TM width is greater than 500 μm [13, 14].

Using SD-OCT, Cheung CY et al. [13] reported that the mean distance from the scleral spur to Schwalbe's line was 670 μm (range: from 390 to 1,230 μm). It is likely that the differences in the present study are due to better visibility of the scleral spur and Schwalbe's line with swept-source OCT. Others have reported on TM width using swept-source OCT, but they defined the TM based on the termination of visible TM using the reflectivity of the structure in SS-OCT images, not on the beginning of Schwalbe's line [14]. Using nasal and temporal quadrants only, the average TM length was 466.9±60.7 μm, but this approach probably misses less clearly visible TM just behind the Schwalbe's line. Deciding exactly where the TM ends in these images is complicated.

Using scanning electron microscopy on histological sections, Spencer described a smooth area called Zone S immediately anterior to the apical portion of TM, encompassing the Schwalbe's ring and the end of Descemet's membrane [15]. This portion varied in length from 50 to 150 μm. Further studies are required to compare in-vivo images with in-vitro high-resolution microscopic images, in order to correlate clinical findings with functional trabecular meshwork boundaries. Recently, Kasuga and associates measured TM width of 158 images from 79 histological slides, and reported that mean TM width was 694.9±109 μm in males and 713.2±106.9 μm in females, lengths that are similar to those found in the present study [16].

The average TM width was significantly shorter in closed-angle than open-angle eyes (P=0.048), in spite of the smaller number of closed-angle eyes included in this study. The apposition of peripheral iris to trabecular meshwork in closed angles may cause image artefacts for the measurement of TM width. Further, we found that the TM width of a particular quadrant was not different between closed and open angles. The TM width was not associated with age, gender, and conventional angle measurements in this study sample. However, further studies with a larger sample size, a wide range of age, ethnicity, and diagnoses are recommended to explore this association of TM width and closed angles.

Although SS was the only visible landmark in time-domain OCT systems, SS, SL, and Schlemm's canal (SC) were visualized with this Fourier-domain OCT [9, 14]. In a previous study, it was possible to locate the SL automatically by using segmentation and edge-detection method [17], and the SL-trabecular iris space area has been proposed as a measure of angle width. Allingham et al. [18] reported that the cross-sectional diameter of SC along the TM ranged from 168 μm to 326 μm in a histopathological study. As the SC is mostly located adjacent to the posterior TM, it is possible to assume this as the approximate width of posterior TM. SC visibility was variable in SS-OCT images in our study. Others reported that SC was visible in SS-OCT high-definition images [9, 14]. Usui T [14] reported that SC was found in 85 % to 90 % of nasal and temporal quadrants. Probably, lower detection rates of the SC in the superior and inferior quadrants resulted in variable visibility of this structure in our study. The knowledge of the measurements of the various structures and their location in relation to the posterior TM using SS-OCT and further refinements of such automated tools may be of relevance in the context of aiding surgical procedures such as angle surgery for glaucoma [14].

Limitations of the current study include the fact that the use of a single grader can result in a systematic bias of the measurements. The correction of refraction distortion of the air–corneal interface may reduce the percentage visibility of Schwalbe's line by compression of the tomogram. It may be improved by averaging of multiple B scans. SS-OCT images were taken at a single meridian or section of a particular quadrant, while the gonioscopic angle grading is typically for the whole quadrant. Finally, image acquisition with the patient looking to the external fixation light at the side of the instrument may potentially change the aqueous dynamics or angle profile compared to the primary gaze position.

In conclusion, the TM width was measurable and reproducible in HD SS-OCT angle images. The inferior TM was the widest compared to other quadrants.

Financial support The study was supported by a Translational Clinical Research Partnership grant from the Biomedical Research Council (BMRC), Singapore.

References

1. Friedman DS, He M (2008) Anterior chamber angle assessment techniques. Surv Ophthalmol 53:250–273
2. Dorairaj S, Liebmann JM, Ritch R (2007) Quantitative evaluation of anterior segment parameters in the era of imaging. Trans Am Ophthalmol Soc 105:99–108
3. Leung CK, Li H, Weinreb RN, Liu J, Cheung CY, Lai RY, Pang CP, Lam DS (2008) Anterior chamber angle measurement with anterior segment optical coherence tomography: a comparison between slit lamp OCT and Visante OCT. Invest Ophthalmol Vis Sci 49:3469–3474
4. Choma M, Sarunic M, Yang C, Izatt J (2003) Sensitivity advantage of swept source and Fourier domain optical coherence tomography. Opt Express 11:2183–2189
5. Fercher AF, Hitzenberger CK, Kamp G, Elzaiat SY (1995) Measurement of intraocular distances by backscattering spectral interferometry. Opt Commun 117:43–48

6. Potsaid B, Baumann B, Huang D, Barry S, Cable AE, Schuman JS, Duker JS, Fujimoto JG (2010) Ultrahigh speed 1050 nm swept source/Fourier domain OCT retinal and anterior segment imaging at 100,000 to 400,000 axial scans per second. Opt Express 18:20029–20048
7. Oh WY, Yun SH, Vakoc BJ, Shishkov M, Desjardins AE, Park BH, de Boer JF, Tearney GJ, Bouma BE (2008) High-speed polarization sensitive optical frequency domain imaging with frequency multiplexing. Opt Express 16:1096–1103
8. Yun S, Tearney G, de Boer J, Iftimia N, Bouma B (2003) High-speed optical frequency-domain imaging. Opt Express 11:2953–2963
9. Leung CK, Weinreb RN (2011) Anterior chamber angle imaging with optical coherence tomography. Eye (Lond) 25:261–267
10. Pavlin CJ, Harasiewicz K, Sherar MD, Foster FS (1991) Clinical use of ultrasound biomicroscopy. Ophthalmology 98:287–295
11. Pavlin CJ, Harasiewicz K, Foster FS (1992) Ultrasound biomicroscopy of anterior segment structures in normal and glaucomatous eyes. Am J Ophthalmol 113:381–389
12. Chan YH (2003) Biostatistics 102: quantitative data—parametric & non-parametric tests. Singapore Med J 44:391–396
13. Cheung CY, Zheng C, Ho CL, Tun TA, Kumar RS, Sayyad FE, Wong TY, Aung T (2011) Novel anterior-chamber angle measurements by high-definition optical coherence tomography using the Schwalbe line as the landmark. Br J Ophthalmol 95:955–959
14. Usui T, Tomidokoro A, Mishima K, Mataki N, Mayama C, Honda N, Amano S, Araie M (2011) Identification of Schlemm's canal and its surrounding tissues by anterior segment fourier domain optical coherence tomography. Invest Ophthalmol Vis Sci 52:6934–6939
15. Spencer WH, Alvarado J, Hayes TL (1968) Scanning electron microscopy of human ocular tissues: trabecular meshwork. Invest Ophthalmol 7:651–662
16. Kasuga T, Chen YC, Bloomer MM, Hirabayashi KE, Hiratsuka Y, Murakami A, Lin SC (2013) Trabecular meshwork length in men and women by histological assessment. Curr Eye Res 38(1):75–79. doi:10.3109/02713683.2012.700757
17. Jing T, Marziliano P, Wong HT (2010) Automatic detection of Schwalbe's line in the anterior chamber angle of the eye using HD-OCT images. Conf Proc IEEE Eng Med Soc [pages 3013–3016]. doi:10.1109/IEMBS.2010.5626167
18. Allingham RR, de Kater AW, Ethier CR (1996) Schlemm's canal and primary open angle glaucoma: correlation between Schlemm's canal dimensions and outflow facility. Exp Eye Res 62:101–109